ACS Macro Letters

Letter

pubs.acs.org/macroletters

Glyco-Inside Micelles and Vesicles Directed by Protection–Deprotection Chemistry

Lu Su,[†] Chenmeng Wang,[†] Frank Polzer,[‡] Yan Lu,[§] Guosong Chen,*[,†] and Ming Jiang*[,†]

[†]The State Key Laboratory of Molecular Engineering of Polymers and Department of Macromolecular Science, Fudan University, Shanghai 200433, China

[‡]TEM Group, Institute of Physics, Humboldt-Universität zu Berlin, 12489 Berlin, Germany

[§]Soft Matter and Functional Materials, Helmholtz-Zentrum Berlin für Materialien und Energie, 14109 Berlin, Germany

Supporting Information

ABSTRACT: Protection–deprotection of carbohydrate is often required in the preparation of glycopolymers, which causes an obvious polarity change of the polymers, but it has been neglected in the studies of self-assembly. In this paper, a new strategy for self-assembly of sugar-containing block copolymers is suggested based on the protection–deprotection chemistry. We found that deacetylation of a series of block copolymers of **PS-*b*-PMan*Ac*** (PS, polystyrene block; PMan*Ac*, "sugar block" with acetylated α-mannopyranoside side groups) in THF resulted in *glyco-inside* structures of the deprotected copolymer **PS-*b*-PMan**, i.e., vesicles with a sugar wall and micelles with a sugar core. Besides, vesicle-to-micelle transition of the assemblies with decreasing the relative length of the sugar block was observed. These unique *glyco-inside* assemblies show interesting functions, such as generating homogeneous Au nanoparticles within the layer of the glyco-block from $AuCl^{4-}$ without any additional reducing reagents or energy input. Control experiments prove that the polar layer of glyco-polymer inside the vesicle provides an essential reduction environment.

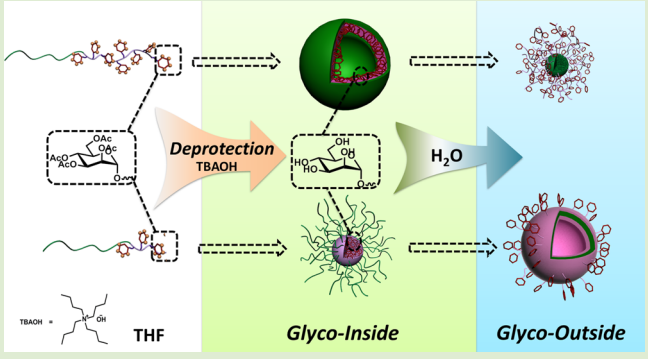

In the long-term studies of self-assembly of biomacromolecules, significant achievements have been made when DNA or proteins serve as the basic building blocks.[1] For example, rigid double-helix DNA could act as the backbone of various assembled tubes and cages with a specific name, "DNA origami", and peptides of α-helix and β-sheet could build the skeleton of various self-assembled structures, for example, the vesicular membrane and fibril backbone. Such self-assembled nanostructures turn out to be very attractive biomimetic and bioinspired materials. Compared to DNA and protein, self-assembly of sugar-containing biomacromolecules is obviously less advanced mainly due to their chemical complexity, diversity, and heterogeneity.[2]

Glycopolymer is one of the most important artificial mimics to glycans in nature due to its feasible preparation and multivalent binding effect.[3] Progress on self-assembly of glycopolymers is also significant in the literature and contributed by several research groups.[4] In these works, glycopolymers always located on the outer layer of nano-objects, i.e., *glyco-outside* structure. However, reports on self-assembled *glyco-inside* structures, i.e., sugars as the "skeleton" of nanomaterials, are very limited. There is only a limited amount of reports using glycopolymer as the major component to build hydrogels.[5] The general strategy to self-assemble glycopolymer in solution is to connect it with a hydrophobic block, either inert or stimulus-responsive, and thus the resultant amphiphile will self-assemble in water.[6] However, this strategy always leads to assemblies with the glycopolymer blocks as the micelle shell acting as a hydrophilic stabilizer just like PEG (poly(ethylene glycol)) or PAA (poly(acrylic acid)) etc. does in various micelles of block copolymers. Thus, contribution from the specificity of the chemical structures of sugars to the assembly process as well as to the characters of the assembled objects has not been systematically investigated.

Herein, the object of this work is aimed at the preparation of *glyco-inside* nanostructures with a new self-assembly strategy. It is well-known that during the synthesis of sugar monomers and oligosaccharides the hydroxyl groups often need to be protected first for performing the subsequent reactions in organic solvents. Therefore, removal of the protective groups is often required to obtain the desired sugar-containing target species. We notice that this protection–deprotection chemistry brings a significant polarity difference in the glycopolymers, which had not been considered in the literature as a driving force for self-assembly of glycopolymers. Our new strategy developed in this paper features fully taking advantage of the

Received: April 8, 2014
Accepted: May 21, 2014
Published: May 23, 2014

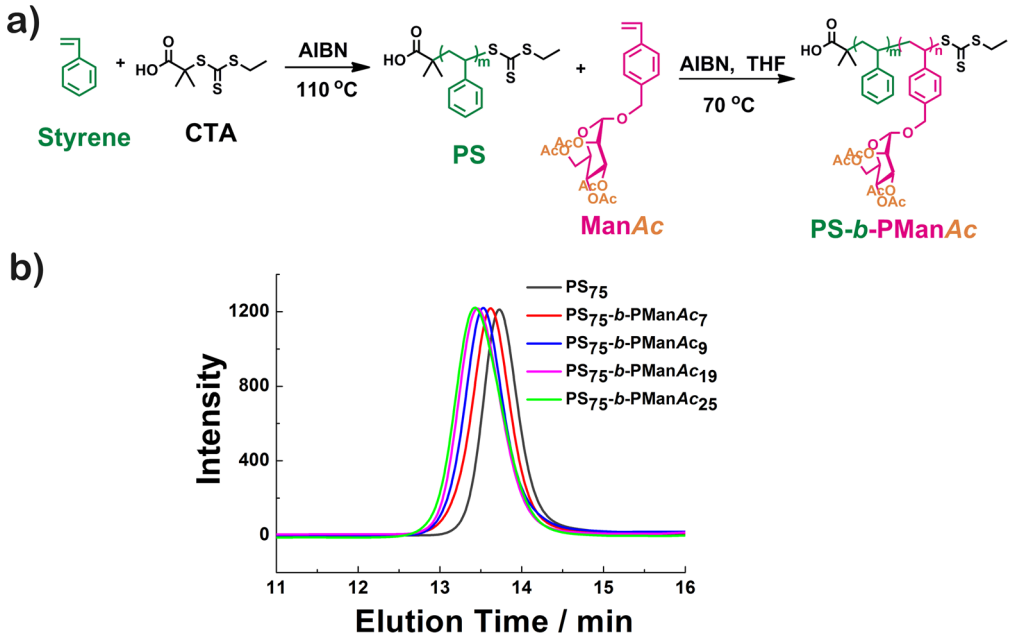

Figure 1. (a) Synthesis of the macro-CTA PS and block copolymers **PS-*b*-PMan*Ac***. (b) GPC curves of **PS-*b*-PMan*Ac*** and the corresponding macro-CTA PS in DMF.

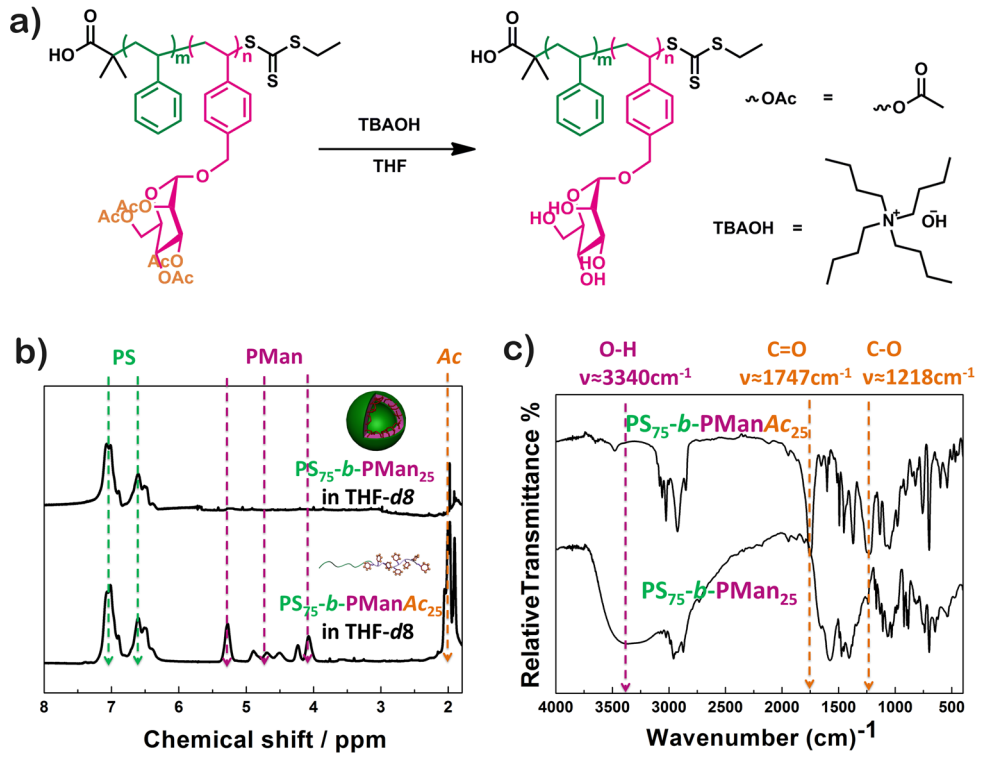

Figure 2. (a) Scheme of deprotection on **PS-*b*-PMan*Ac*** to form **PS-*b*-PMan** and the chemical structure of the catalyst. (b) ^{1}H NMR spectra of **PS$_{75}$-*b*-PMan*Ac*$_{25}$** and **PS$_{75}$-*b*-PMan$_{25}$** in THF-d_8 at room temperature (peaks from solvents were removed for clarity). (c) FT-IR spectra of **PS$_{75}$-*b*-PMan*Ac*$_{25}$** and **PS$_{75}$-*b*-PMan$_{25}$**.

necessary protection−deprotection steps in the preparation of sugar-containing polymers to drive their assembly, resulting in the desired nanosized *glyco-inside* objects, i.e., micelles with a sugar core and vesicles with a sugar center layer. This new strategy can be regarded as an important development of "chemical reaction-induced micellization" of block copolymers.[7]

To demonstrate this deprotection-induced micellization of sugar-containing polymers, block copolymers composed of one sugar block with protective groups on their glyco-units and a hydrophobic block are designed. Polystyrene (PS) was chosen as the hydrophobic block, which is inert to hydrogen bonding. For the glyco-monomer, tetra-acyl-α-1-mannosyl styrene (Man*Ac*) was synthesized according to the reported procedure (synthetic steps and characterizations are in the Supporting Information).[8] The block copolymer **PS-*b*-PMan*Ac*** (PMan*Ac*: poly(Man*Ac*)) was obtained via two-step RAFT (reversible

dx.doi.org/10.1021/mz500211v | *ACS Macro Lett.* 2014, 3, 534−539

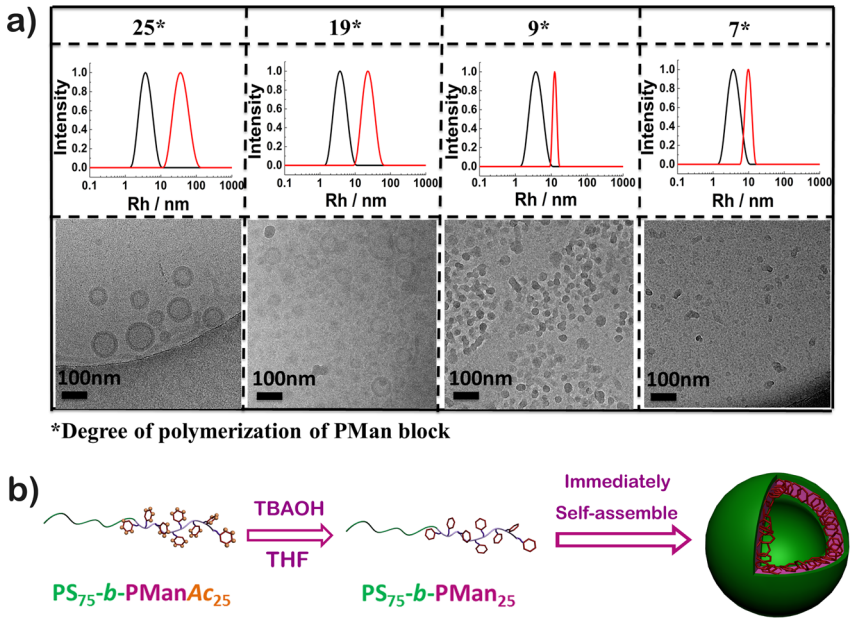

Figure 3. (a) $\langle R_h \rangle$ distributions of **PS$_{75}$-*b*-PMan*Ac*** (black) and **PS$_{75}$-*b*-PMan** (red) in THF after CONTIN analysis and cryo-TEM images of the self-assemblies in THF. (b) Scheme of the deprotection-induced micellization (vesicles) process.

addition−fragmentation chain transfer) polymerization (Figure 1a). Briefly, the PS block was first synthesized in the presence of *S*-ethyl-*S*′-(*α*,*α*′-dimethyl-*α*″-acetic acid) trithiocarbonate, which was then used as a macro-CTA (chain transfer reagent) to initiate the monomer Man*Ac*. A series of block copolymers with different PMan*Ac* block length from the identical PS macro-CTA (degree of polymerization 75) were prepared. GPC traces of macro-CTA PS and the block copolymers **PS$_{75}$-*b*-PMan*Ac*$_n$** (n = 7, 9, 19, 25) are shown in Figure 1b. PDI (less than 1.10) and Mn obtained from GPC and ^{1}H NMR (Figures S1−S5) are listed in Table S1 (Supporting Information).

There are varieties of deprotection catalysts for the removal of *O*-acetyl protecting groups on carbohydrates, but for performing the deprotection-induced self-assembly and monitoring the process by DLS (dynamic light scattering) and TEM (transmission electronic microscopy), most of the common deprotection catalysts could not be utilized. For example, although sodium methoxide in methanol for well-known "Zémplen decacetylation" is the most common one,[9] it formed particles in the nano- or microscale in most organic solvents (Figure S6, Supporting Information), which made DLS and TEM analysis impractical. Similarly, potassium carbonate was proved not suitable either. Organic amines, e.g., triethylamine, do not bring such problems, but the required amount of amines for sufficient deprotection was too large due to their relatively weak catalytic ability resulting in a substantial change in the solvent property, which might influence the deprotection process. Finally, we found that tetrabutylammonium hydroxide (TBAOH) in water matched the requirements and served well as an effective and soluble catalyst in THF (Figure 2). The minimal amount of the catalyst (6 μL of 40% TBAOH in water vs 1 mg of Man*Ac*) was estimated by a model reaction (Figure S7, Supporting Information). It is worth mentioning that this is the first time using TBAOH for deacylation of polymers and small molecules as well, and this reagent was found to be critical to the success of self-assembly.

^{1}H NMR and FT-IR were employed to demonstrate the removal of the acetyl groups of the protected block copolymers under the catalysis of TBAOH. The data for **PS$_{75}$-*b*-PMan*Ac*$_{25}$** are shown in Figure 2 as an example. For the copolymer in THF-d_8 before deacylation (Figure 2b and Figure S8, Supporting Information), peaks around δ = 4.0−5.5 ppm clearly showed the pyranose ring of the sugars, and those around δ = 6.3−7.3 ppm showed the phenyl groups in both PS block and glyco-block. Meanwhile, peaks around δ = 2.0 ppm confirmed the presence of acetyl groups on the sugar backbone. Once TBAOH was added, the signals of the acetyl groups almost disappeared since most of the byproduct TBAO*Ac* was trapped inside the hydrophilic part, showing the successful removal of the groups and the formation of unprotected **PS$_{75}$-*b*-PMan$_{25}$**. Moreover, in the FT-IR results, a significant enhancement of the characteristic broad absorption of hydroxyl groups at ν = 3340 cm^{-1} and disappearance of the signals of acetyl groups at 1747 (ν(C═O)) and 1218 cm^{-1} (ν(C−O)) (Figure 2c and Figure S8, Supporting Information) also supported the formation of **PS$_{75}$-*b*-PMan$_{25}$** from **PS$_{75}$-*b*-PMan*Ac*$_{25}$** after treatment of TBAOH. In particular, after the deprotection, the NMR signals of the pyranose rings disappeared, and those of the phenyl groups slightly decreased (Figure 2b). Considering that the number of phenyl groups of the sugar block is much smaller than that of the PS block, the NMR results can be attributed to the sugar block transforming from the soluble state to less solvated. This implies the self-assembly of the block copolymer in THF as a result of the deprotection. A similar conclusion was made for the other block copolymers **PS$_{75}$-*b*-PMan*Ac*$_n$** (n = 19, 9, 7) based on the corresponding results of ^{1}H NMR and FT-IR (Figures S9−S11, Supporting Information).

DLS and TEM were further conducted to monitor and confirm the self-assembly caused by deacylation. As expected, the block copolymer **PS$_{75}$-*b*-PMan*Ac*$_{25}$** (2 mg/mL) existed as a single chain with a very small $\langle R_h \rangle$ (hydrodynamic radius) of 3 nm in THF (Figure 3a). Once 20 μL of TBAOH aqueous solution was added into the 3 mL THF solution of **PS$_{75}$-*b*-PMan*Ac*$_{25}$**, blue opalescence appeared immediately, accompanied by an increase of $\langle R_h \rangle$ from 3 to 42 nm (Figure 3a),

dx.doi.org/10.1021/mz500211v | *ACS Macro Lett.* 2014, 3, 534−539

Table 1. Summary of $\langle R_h \rangle$, PDI, and Morphology of the Self-Assembled Structures in THF and Water[a]

	in THF					in water		
self-assembly polymer	$\langle R_h \rangle$/nm	PDI	$\langle R_g \rangle$/nm	$\langle R_g \rangle/\langle R_h \rangle$	morphology	$\langle R_h \rangle$/nm	PDI	morphology
PS_{75}-*b*-$PMan_{25}$	42	0.12	40.3	0.96	v	11	0.08	m
PS_{75}-*b*-$PMan_{19}$	25	0.09	26	1.04	v	12	0.07	m
PS_{75}-*b*-$PMan_{9}$	13	0.08	8.6	0.66	m	60	0.35	m and v
PS_{75}-*b*-$PMan_{7}$	10	0.1	6.8	0.68	m	102	0.15	v

[a]m: micelle. v: vesicle ($\langle R_h \rangle$, $\langle R_g \rangle$, and PDI were determined by DLS and SLS (Figure S12, Supporting Information)).

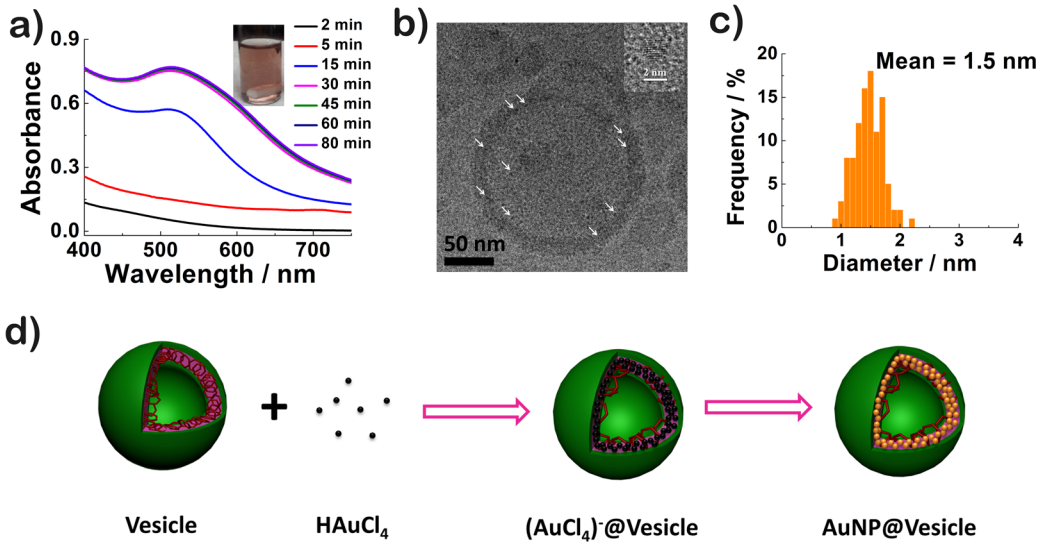

Figure 4. (a) Evolution of UV–vis spectra after mixing of **PS_{75}-*b*-$PMan_{25}$** aggregates with $HAuCl_4$ at 25 °C. ([$HAuCl_4$] = 0.2 mM, [$HAuCl_4$]:[PS_{75}-*b*-$PMan_{25}$] = 2:1; inset: photo of the reaction vial). (b) Cryo-TEM image of **PS_{75}-*b*-$PMan_{25}$** with AuNPs (inset: the enlarged AuNP under HR-TEM). (c) Particle size distribution of AuNPs formed inside the vesicle membrane of **PS_{75}-*b*-$PMan_{25}$** (number of NPs measured: 100). (d) Proposed scheme of formation of AuNPs inside within the vesicle membrane.

which clearly indicated the formation of self-assembled structures. Moreover, the ratio of $\langle R_g \rangle/\langle R_h \rangle$ ($\langle R_g \rangle$: radius of gyration from static light scattering, SLS) was measured as 0.96 (Table 1), a characteristic value of vesicles. The cryo-TEM image confirmed the morphology of vesicles with a diameter of 90 nm and its membrane thickness of 10 nm (Figure 3a), which was consistent with the $\langle R_h \rangle$ measured by DLS. Combined with the information from the ^{1}H NMR spectrum (Figure 2b), i.e., the disappearance of signals from the pyranose ring of sugars in THF-d_8, the vesicle membrane can be deduced as a sandwich structure with the glyco-block as the middle layer and PS as the outer and inner layer. Moreover, all of the other block copolymers **PS_{75}-*b*-$PManAc_n$** (n = 19, 9, 7) showed similar self-assembly behavior after deacylation, forming vesicles or micelles with *glyco-inside* structures. All the related data from DLS and SLS and cryo-TEM are shown in Figure 3a and Table 1. Similar to **PS_{75}-*b*-$PManAc_{25}$**, the copolymer with a relatively long sugar block, i.e., **PS_{75}-*b*-$PManAc_{19}$**, formed vesicles as well, as judged by the cryo-TEM image (Figure 3a) and the value of $\langle R_g \rangle/\langle R_h \rangle$ = 1.04 (Table 1). However, the two copolymers with shorter sugar blocks, i.e., **PS_{75}-*b*-$PManAc_9$** and **PS_{75}-*b*-$PManAc_7$**, led to core–shell micelles as observed by cryo-TEM and supported by DLS of much smaller size, 13 and 10 nm, and lower $\langle R_g \rangle/\langle R_h \rangle$ of 0.66 and 0.68, respectively. In short, all the data led to the attractive feature of the assemblies; i.e., with increasing length of the sugar-containing block, which is the solvophobic one in THF, the morphology transition from the vesicle to the micelle takes place. This is in agreement with the general theory of morphology change with the "packing parameter", which was determined by the relative length or volume of the solvophilic and solvophobic blocks.[10] Such a simple rule was found true for many amphiphilic block copolymers, particularly the block copolymer PAA-*b*-PS.[11] It is worth mentioning that each sugar-containing unit is much larger than that of the PS unit, so even when the lengths of $PMan_{25}$ and $PMan_{19}$ are lower than that of PS_{75}, they lead to vesicles.

New functions of such *glyco-inside* vesicles and micelles are expected and worth exploring. The first attempt in this respect was in fabricating gold nanoparticles (AuNPs) via reduction of chloroauric acid. In the literature, various procedures were reported to prepare hybrid AuNPs via chemical reduction and/or light irradiation,[12] in some of which sugar-decorated polymers or dendrimers were involved.[13] These procedures were proved successful; however, a reducing reagent was always necessary to obtain regular particles with relatively small size. Herein our *glyco-inside* assembled objects were found to be a good platform to produce AuNPs with some advantages. As shown in Figure 4a, after addition of $HAuCl_4$ (0.2 mM) to the vesicle solution of **PS_{75}-*b*-$PMan_{25}$** in THF, an absorption band at around 510 nm appeared, showing the formation of AuNPs. The optical intensity at 510 nm increased sharply at the first 30 min and then reached a maximum, indicating completion of the reduction. In addition, the photo of the reaction vial clearly showed the well-dispersed AuNPs in THF (Figure 4a, inset). The cryo-TEM image (Figure 4b) showed that the AuNPs in fact are located inside the vesicle membrane. Compared to the cryo-TEM image of **PS_{75}-*b*-$PMan_{25}$** vesicles before hybrid-

dx.doi.org/10.1021/mz500211v | ACS Macro Lett. 2014, 3, 534–539

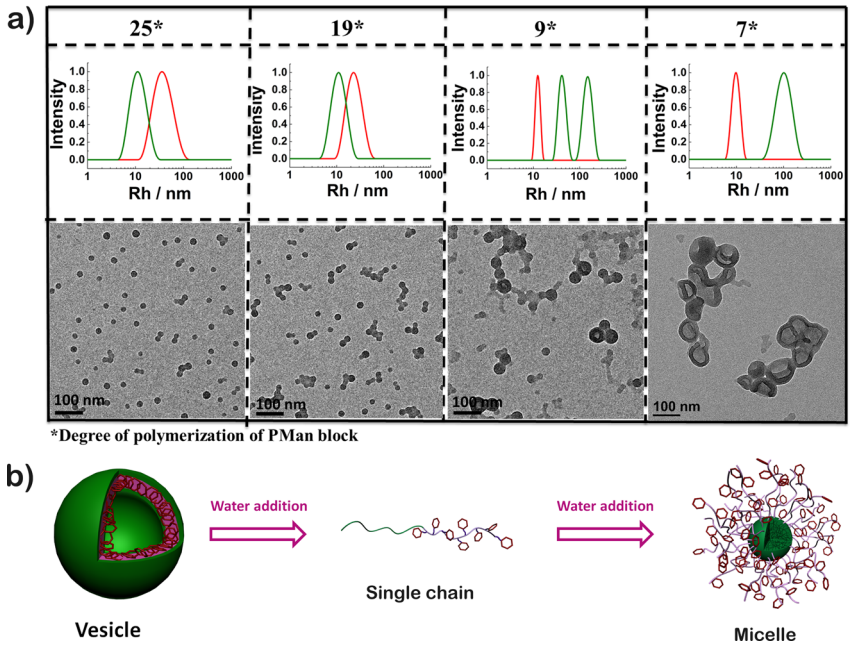

Figure 5. (a) $\langle R_h \rangle$ distribution and TEM images of $\mathbf{PS_{75}}$-*b*-$\mathbf{PMan_n}$ in water, where n = 25 and 19 show micelles, n = 9 shows the coexistence of micelles and vesicles, and n = 7 shows vesicles. (b) Proposed mechanism of inversion of the *glyco-inside* vesicles to *glyco-outside* micelles after addition of water.

ization (Figure 3a), the vesicle in Figure 4b exhibits a higher contrast due to the membrane being decorated with the black dots of AuNPs (some are pointed by white arrows). HR-TEM confirmed the formation of AuNPs by revealing its crystal lattice (Figure 4b inset). Interestingly, the AuNPs generated quickly (<0.5 h) are small with an average diameter of 1.5 nm only and nearly monodispersed (Figure 4c). Such a narrow size distribution for such a small size of AuNPs prepared without any additional reductant has seldom been reported before. Moreover, the average diameter depends on the glyco-block length; the diameter of AuNPs from $\mathbf{PS_{75}}$-*b*-$\mathbf{PMan_7}$ with the shortest sugar block was around 2.7 nm (Figure S13, Supporting Information).

As the reduction of $HAuCl_4$ to AuNPs here was realized without any additional reducing reagent and energy input, our *glyco-inside* vesicles and micelles could be regarded as a "green microreactor" producing small and narrow-distributed AuNPs. We hypothesized that when the precursor $HAuCl_4$ was added it would move to the hydrophilic glyco-block membrane or core where the high local concentration of sugar units benefits the reduction.[14] Furthermore, the solidified glyco-block membrane or core would restrict the mobility of the nascent Au clusters preventing their aggregation, which of course results in a narrow size distribution.[15] In addition, the AuNPs formed in such a procedure were well-dispersed in aqueous dispersion when the medium was switched from THF to water (Figure S14, Supporting Information).

The self-assembled *glyco-inside* structures can be further inversed to *glyco-outside* structures. To the vesicle solution of $\mathbf{PS_{75}}$-*b*-$\mathbf{PMan_{25}}$ in THF, addition of water up to 15 wt % led to destruction of the vesicles as evidenced by a dramatic decrease of the scattered light intensity (Figure S15, Supporting Information) and disappearance of the blue opalescence. Upon further increase of the water content to 27 wt % and more, another self-assembled object with much smaller $\langle R_h \rangle$, approximately 11 nm, appeared, which was found to be a micelle by TEM (Figure 5a). Results from the ^{1}H NMR spectrum (Figure S8, Supporting Information), i.e., reappearance of the signals from the pyranose ring of sugars (δ = 3.0–4.0 ppm) and almost disappearance of the signals from the phenyl group in water, indicated that the micelles obtained in water contain PS as the core and glyco-block as the shell. Similarly, after addition of water, the self-assembled structures formed by $\mathbf{PS_{75}}$-*b*-$\mathbf{PMan_n}$ (n = 19, 9, 7) also showed the distinctive inversion (Figures S9–S11, Supporting Information). The related light scattering data and cryo-TEM images are shown in Figure 5a. It is noticed that similar to $\mathbf{PS_{75}}$-*b*-$\mathbf{PMan_{25}}$ the *glyco-inside* vesicles of $\mathbf{PS_{75}}$-*b*-$\mathbf{PMan_{19}}$ in THF were converted to *glyco-outside* micelles in water, and the opposite morphology change from micelle to vesicle was observed for the block copolymers with the short sugar blocks, i.e., $\mathbf{PS_{75}}$-*b*-$\mathbf{PMan_9}$ and $\mathbf{PS_{75}}$-*b*-$\mathbf{PMan_7}$. It is very interesting to see that in this process of switching THF to water what we observed is the concommitance of *glyco-inside* to *glyco-outside* inversion and the transformation between vesicles and micelles. Besides, the data in Figure 5a show that with decreasing the relative lengths of the solvophilic block, i.e., the sugar block in water, the aggregate morphology changes from micelles to vesicles. This result is also in good agreement with the theoretical expectations.[10]

Finally, aggregation and dissociation of the reversed nanostructures with glycopolymer as the shell can be further manipulated with Ca^{2+}. It is known that Ca^{2+} can induce carbohydrate–carbohydrate interactions between polysaccharides.[16] In the current case, we find that the effectiveness of addition of Ca^{2+} strongly depends on the length of the glyco-block. For $\mathbf{PS_{75}}$-*b*-$\mathbf{PMan_{25}}$ (0.4 mg/mL), after Ca^{2+} (5 mM) was added, the $\langle R_h \rangle$ increased gradually (Figure S16, Supporting Information), and precipitation was observed within 0.5 h, which was also visualized under TEM (Figure S17, Supporting Information). This interaction was proved reversible upon dialysis against water (Figure S18, Supporting

dx.doi.org/10.1021/mz500211v | *ACS Macro Lett.* 2014, 3, 534–539

Information). However, for PS_{75}-*b*-$PMan_7$ with a much shorter sugar block, no change of $\langle R_h \rangle$ was observed for at least 2 days after Ca^{2+} addition by DLS (Figure S19, Supporting Information) and TEM (Figure S20, Supporting Information).

■ ASSOCIATED CONTENT

Supporting Information

Synthesis and characterization of monomer Man*Ac*, block copolymer PS-*b*-PMan*Ac*, and PS-*b*-PMan including ^{1}H NMR as well as details of DLS, TEM, and UV−vis spectroscopy measurements. This material is available free of charge via the Internet at http://pubs.acs.org.

■ AUTHOR INFORMATION

Corresponding Authors

*E-mail: guosong@fudan.edu.cn
*E-mail: mjiang@fudan.edu.cn.

Notes

The authors declare no competing financial interest.

■ ACKNOWLEDGMENTS

Ministry of Science and Technology of China (2011CB932503), National Natural Science Foundation of China (No. 91227203, 51322306), Innovation Program of Shanghai Municipal Education Commission, and Shanghai Rising-Star Program (Grant 13QA1400600) are acknowledged for their financial support.

■ REFERENCES

(1) (a) Rodriguez-Hernandez, J.; Lecommandoux, S. *J. Am. Chem. Soc.* **2005**, *127*, 2026−2027. (b) Aldaye, F. A.; Palmer, A. L.; Sleiman, H. F. *Science* **2008**, *321*, 1795−1799. (c) Hamley, I. W. *Angew. Chem., Int. Ed.* **2007**, *46*, 8128−8147. (d) Wang, R.; Xu, N.; Du, F. S.; Li, Z. C. *Acta. Polym. Sin.* **2013**, *6*, 774−780.

(2) (a) Zhao, Y.; Sakai, F.; Su, L.; Liu, Y.; Wei, K.; Chen, G.; Jiang, M. *Adv. Mater.* **2013**, *25*, 5215−5256. (b) Chen, G. S. *Prog. Chem.* **2010**, *22*, 1753−1759.

(3) (a) Mammen, M.; Choi, S. K.; Whitesides, G. M. *Angew. Chem., Int. Ed.* **1998**, *37*, 2755−2794. (b) Pfaff, A.; Shinde, V. S.; Lu, Y.; Wittemann, A.; Ballauff, M.; Muller, A. H. E. *Macromol. Biol.* **2011**, *11*, 199−210.

(4) (a) Kumar, J.; Bousquet, A.; Stenzel, M. H. *Macromol. Rapid Commun.* **2011**, *32*, 1620−1626. (b) Cameron, N. R.; et al. *Faraday Discuss.* **2008**, *139*, 259−368.

(5) Sakamoto, N.; Suzuki, K.; Kishida, A.; Akashi, M. *J. Appl. Polym. Sci.* **1998**, *70*, 965−972.

(6) (a) Pasparakis, G.; Alexander, C. *Angew. Chem., Int. Ed.* **2008**, *47*, 4847−4850. (b) You, L. C.; Schlaad, H. *J. Am. Chem. Soc.* **2006**, *128*, 13336−13337. (c) Su, L.; Zhao, Y.; Chen, G.; Jiang, M. *Polym. Chem.* **2012**, *3*, 1560−1566. (d) Huang, J.; Bonduelle, C.; Thévenot, J.; Lecommandoux, S.; Heise, A. *J. Am. Chem. Soc.* **2012**, *134*, 119−122.

(7) (a) Wu, C.; Niu, A. Z.; Leung, L. M.; Lam, T. S. *J. Am. Chem. Soc.* **1999**, *121*, 1954−1955. (b) Chen, D. Y.; Peng, H. S.; Jiang, M. *Macromolecules* **2003**, *36*, 2576−2578. (c) Ladmiral, V.; Semsarilar, M.; Canton, I.; Armes, S. P. *J. Am. Chem. Soc.* **2013**, *135*, 13574−13581.

(8) Narumi, A.; Kaga, H.; Kawasaki, K.; Taniguchi, Y.; Satoh, T.; Kakuchi, T. *J. Polym. Sci. A: Polym. Chem.* **2001**, *39*, 4061−4067.

(9) Zemplen, G.; Pacsu, E. *Ber. Dtsch. Chem. Ges.* **1929**, *62*, 1613−1614.

(10) Isrealachvilli, J. N.; Marcelja, S.; Horn, R. G. *Q. Rev. Biophys.* **1980**, *13*, 121−200.

(11) Mai, Y.; Eisenberg, A. *Chem. Soc. Rev.* **2012**, *41*, 5969−5985.

(12) (a) Cai, H. X.; Yao, P. *Nanoscale* **2013**, *5*, 2892−2900. (b) Kurihara, K.; Kizling, J.; Stenius, P.; Fendler, J. H. *J. Am. Chem. Soc.* **1983**, *105*, 2574−2579.

(13) (a) de la Fuente, J. M.; Barrientos, A. G.; Rojas, T. C.; Rojo, J.; Cañada, J.; Fernández, A.; Penadés, S. *Angew. Chem., Int. Ed.* **2001**, *40*, 2257−2261. (b) Housni, A.; Cai, H.; Liu, S.; Pun, S. H.; Narain, R. *Langmuir* **2007**, *23*, 5056−5061. (c) Esumi, K.; Suzuki, A.; Aihara, N.; Usui, K.; Torigoe, K. *Langmuir* **1998**, *14*, 3157−3159.

(14) (a) Raveendran, P.; Fu, J.; Wallen, S. L. *J. Am. Chem. Soc.* **2003**, *125*, 13940−13941. (b) Liu, J.; Anand, M.; Roberts, C. B. *Langmuir* **2006**, *22*, 3964−3971.

(15) Esumi, K.; Hosoya, T.; Suzuki, A.; Torigoe, K. *Langmuir* **2000**, *16*, 2978−2980.

(16) (a) Reynolds, A. J.; Haines, A. H.; Russell, D. A. *Langmuir* **2006**, *22*, 1156−1163. (b) Bucior, I.; Burger, M. M. *Curr. Opin. Struct. Biol.* **2004**, *14*, 631−637.